Korea-Australia Rheology Journal
Vol. 20, No. 1, March 2008 pp. 7-14

Numerical and experimental analysis of the resin transfer molding process

Mohamed Hattabi[1,*], Jamal Echaabi[1,*] and Mohamed Ouadi Bensalah[2,*]
[1]*Equipe de Recherche Appliquée sur les Polymères, Département de Génie Mécanique, ENSEM, Université Hassan II Aïn Chock, BP 8118, Oasis, Casablanca, Maroc.*
[2]*Laboratoire de mécanique et des matériaux Avenue Inb Batouta BP 1014, Faculté des sciences, Rabat, Maroc*
(Received Mar. 18, 2007; final revision received Jan. 6, 2008)

Abstract

The objective of this work is to propose a procedure to simulate the flow in the LCM (Liquid Composites Molding) processes by finite difference discretization in a curvilinear coordinate system adapted to the shape of the saturated zone. The numerical results obtained are compared with experimental results obtained by an experimental device elaborated at our laboratory. It allows to realize linear and radial injections for different porosities and to observe the flow front kinetics. Numerical and experimental results are then compared with those of the literatures and excellent agreements are noticed. Finally, we suggest a concept of the capillary number to explain the variations of the permeability obtained for pressure values lower than 0.25 Bar.

keywords : liquid composites moulding, numerical simulation, flow front and void, capillary pressure

1. Introduction

Liquid composites molding (LCM) processes are becoming more and more popular in the industry. One of this class of manufacturing processes is the injection with closed mold called RTM (Resin Transfer Molding). Liquid composites molding (LCM) consists of the injection of a thermoset resin in a closed mold containing a fibrous reinforcement of glass or carbon fibers. The present study concerns the numerical simulation and experimental investigation of (LCM) processes. The numerical methods developed in the literatures are based on a finite element approach coupled with control volume (Bruschke and Advani, 1990; Gauvin and Trochu, 1993; Young *et al.*, 1991; Liu, 2000; Shojaei *et al.*, 2002). This type of approach seems well adapted to the complex geometries of fabricated structures. However, it leads to a discrepancy in tracking exact position of the flow front during the mold filling unless a numerical mesh is regenerated along the flow advancement at every time step. On the other hand, in the present work, we adopt a numerical method of finite difference scheme with a curvilinear mesh system, which describes better the progress of the resin flow front, by remeshing the saturated part of the mold during the mold filling process (Hattabi *et al.*, 2005).

The knowledge of the permeability of fibrous reinforcements is indispensable to the simulation of the RTM process. An experimental apparatus to study linear and radial flows is devised. We measure the permeability according to the parameters of the process control and present the expression of the capillary number and of the critical length for linear and radial flows. Measurements are made for a radial injection by a simple technique. Through the analysis of the flow front kinetics, the permeability tensor is identified. The results of the measurement and the examination of the capillary number clarify the existence of a non-saturated zone which can be characterized by a critical length. The governing equations of problem and their solutions, the experimental device and the modeling of the capillary effect are presented.

2. The proposed technique

The purpose of this study is to simulate two-dimensional mold filling of Newtonian fluid through the porous reinforcement under an isothermal condition. It is supposed that the fluid is incompressible, the gravitational force is negligible and the surface effects in the mold walls are neglected in front of the resistance in the porous media as well as the capillarity effect and of wetting fibers in front of the pressures of flow.

In the macroscopic scale, the resin flow through a fibrous reinforcement is described by the continuity equation and Darcy's law:

$$div(\vec{V}) = 0 \tag{1}$$

$$\vec{V} = -\frac{\overline{\overline{K}}}{\mu} grad(\vec{P}) \tag{2}$$

*Corresponding author: M. Hattabi (mohamedhattabi@hotmail.com)
J. Echaabi (j.echaabi@ensem-uh2c.ac)
M.O. Bensalah (bensal@hotmail.com)

where: $\vec{V}$, μ, $grad(\vec{P})$ and $\overline{\overline{K}}$ represent respectively, the velocity vector, the resin viscosity, the pressure gradient and the permeability tensor. The interest of our work is to follow the flow front in the planar principal directions. In that case $\overline{\overline{K}}$ is :

$$\overline{\overline{K}} = \begin{bmatrix} K_x & 0 \\ 0 & K_y \end{bmatrix} \tag{3}$$

The substitution of the Eq. (2) and (1) gives:

$$\frac{\partial}{\partial x}\left(\frac{K_x \partial P}{\mu \partial x}\right) + \frac{\partial}{\partial y}\left(\frac{K_y \partial P}{\mu \partial y}\right) = 0 \tag{4}$$

The simulation of the mold filling is performed by the numerical solution of the elliptic Eq. (4) for pressure fields, associated with boundary conditions taken as follows: at the injection gates $P = P_{inj.}$ or $Q = Q_{inj.}$ where $P_{inj.}$ and $Q_{inj.}$ are the pressure and the flow rate of the injection respectively. At the impermeable mold wall $\partial P/\partial n = 0$ and at the flow front $P_{front} = P_{atmosphere}$.

3. Procedure of numerical simulation

Major difficulty in this problem does not lie in the numerical solution of the elliptic Eq. (4), but rather in the fact that the geometry of the calculation domain varies with the time. Indeed, at every time step, we must solve this equation in the saturated part of the mold. A spatial discretization by means of a curvilinear coordinate system is chosen and then adapted to the complex shape of the domain where lines of the mesh coincide with the material front and the line of injection. If $\xi(x,y)$ and $\eta(x,y)$ represent the network of the lines of the mesh, such an elliptic coordinate system can be obtained by solution in the saturated zone. According to (Saouab, 1991):

$$\Delta\xi(x,y) = P;\ \Delta\eta(x,y) = Q \tag{5}$$

With conditions in limits translating the passage of lines of meshing on the edge of the saturated zone, functions P and Q allow the mastery of the control of the spacing in the meshing. In these conditions, we can see that the solution of the system (5) is equivalent to the solution in an oblong domain R of the elliptic quasi-linear system (Hattabi *et al.*, 2005):

$$AX_{\xi\xi} + BX_{\eta\eta} + 2CX_{\xi\eta} = -J^2(PX_{\xi} + QX_{\eta}) \tag{6}$$

where:

$X = (x,y)^T$, $J = x_{\xi}y_{\eta} - x_{\xi}y_{\eta}$,

$A = |X_{\eta}|^2$, $B = |X_{\xi}|^2$ *and* $C = X_{\xi}X_{\eta}$.

Boundary conditions are given by the specification of the borders of the saturated zone. Although the shape of this system is more complicated than that of the system of Poisson Eq. (5), the boundary conditions are formulated along the rectilinear borders of the oblong domain. The discretization is easily performed on a Cartesian network and leads to generate a curvilinear coordinate system adapted to the geometry of the saturated region. The discretization of Eq. (4) is realized on the nodes of the mesh obtained by central finite difference schemes. The equation is solved by means of an iterative method using successive relaxation. The obtained pressure distribution is used with Darcy's law (2) to estimate the velocity of the flow front and to determine its new position at every step of time. Even though, if completion is not a steady state process, quasi-steady state is assumed and it is feigned so by a succession of permanent states taken on increments of relatively small times. A new distribution of nodes for the new position of the front is adopted according to its length and to its shape. Then a mesh is again regenerated. This sequence continues until the mold is completely filled. Obtained results will be presented after the description of the experimental device.

4. Experimental device

The experimental device is used to perform a radial injection. The mold consists of a steel bottom and Plexiglass top plaques. Injection is done by means of a buzzard placed at the centre of the mold and connected with a jack by a flexible hose equipped with a distributor to evacuate air bubbles. The hydraulic jack containing the glycerin is activated by a drive machine. The fluid permeates through the reinforcement placed inside the mould cavity in the bidirectional flow (2D), before the air exits completely from the mold through the vents placed on the bottom of the mold. The technique of radial injection has some advantages on the measurement of the unidirectional permeability. It allows to make a single measurement of the permeability tensor and to eliminate the edge effects usually met in the unidirectional techniques of measurement of permeability. Using the experimental set up, the evolution of the flow front with the time is observed and the drop of injection pressure is measured between two successive positions of the front. The measurement of the injection pressure is performed by a pressure sensor placed exactly at the point of injection. A transparent upper patch containing several circles of various diameters and lines with various angles is used to measure the radius of the flow front (Fig. 1 and 2) during the filling.

Injection is done by a bronze injector designed to prevent some experimental problems (Gouley, 1995). With this device, the progress of the flow front is captured and saved by a digital camera. The images saved by this camera are digitized and transferred to a computer. On the images at various intervals of time, the points on the circumference of the circle are identified with their coordinates. Isotropic reinforcements of different porosities are used in this study. The tests are realized by means of a non reactive fluid, the

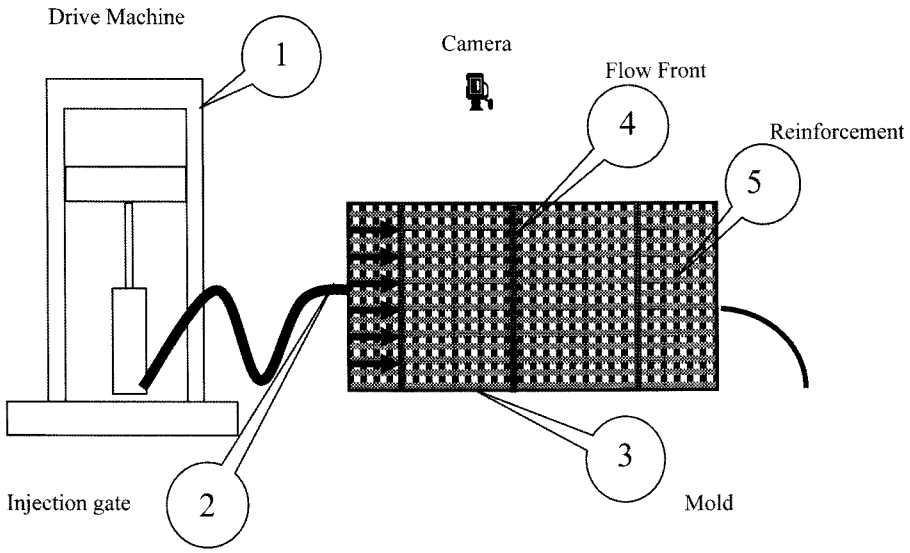

Fig. 1. Experimental device for linear injection (1D).

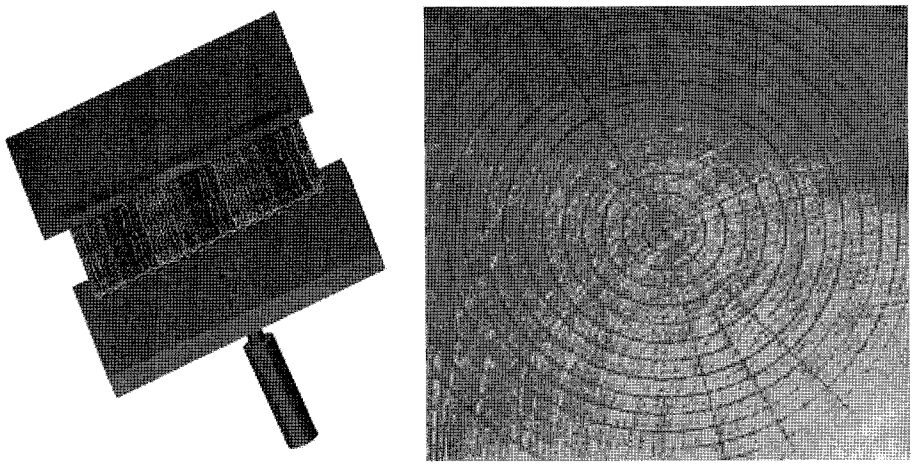

Fig. 2. Mold parts and system of measurement for radial injection (2D).

glycerin whose viscosity is of the order of 1 Pa.s at the ambient temperature (20°C). This fluid is diluted with some distilled water so that the viscosity of systems is met in the usual application of the process. The viscosity of this fluid is measured with a Brook field type viscometer.

5. Results and discussions

5.1. Validations

In the first application, we consider a rectangular cavity in which a reinforcement of isotropic permeability K and of porosity ϕ is placed. Then a resin of viscosity (μ) is injected in the rectangular cavity of the mold under a constant injection pressure P_{inj}. The front progresses then in a straight shape perpendicular to the direction of flow (direction Ox) and linear injection flow is realized. In these conditions, the kinetics of the flow front can be obtained analytically as follows:

$$x_f(t) = \sqrt{\left(\frac{2KP_{inj}}{\phi\mu}t\right)} \tag{7}$$

in the first example, we compare our numerical results with analytical results (Eq. (7)) and with other numerical results (Shojaei *et al.*, 2002). Here, the resin is injected under the pressure of $P_{inj} = 1.5\ 10^5\ Pa$ through an isotropic reinforcement, the ratio of the permeability to the viscosity is $K/\mu = 300\ mm^2/mPa{\cdot}s$ and the porosity $\phi = 0.4$. Fig. 3 presents the comparison of the flow front kinetics.

In the second application, an anisotropic reinforcement of porosity $\phi = 0.453$ is considered and the flow progression is recorded in the principal directions noted Ox and Oy associated to the direction of warp and weft of the weaving of this reinforcement. The permeability tensor $\overline{\overline{K}}$ is diagonal with $K_x = 2\ 10^{-11}\ m^2$ and $K_y = 2\ 10^{-12}\ m^2$. The resin with a viscosity of $\mu = 0.109\ Pa{\cdot}s$, is injected under a pressure of $P_{inj} = 2.035\ 10^5\ Pa$ by an injection gate whose

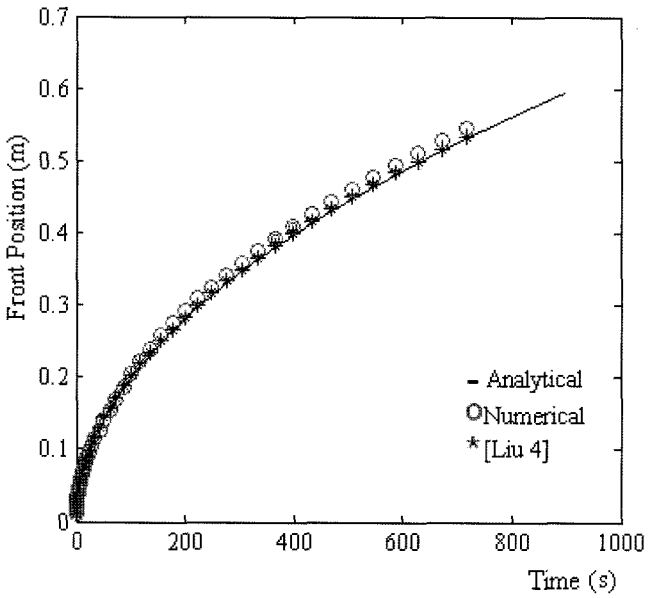

Fig. 3. Comparison of the flow kinetics.

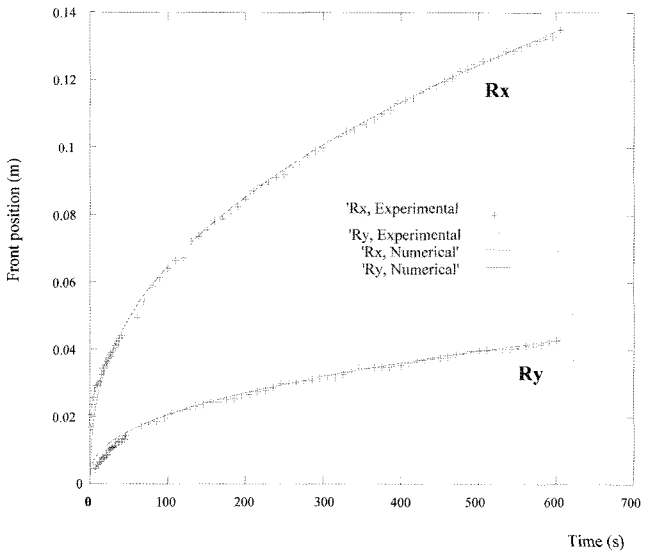

Fig. 4. Comparison between numerical and experimental flow front for two radius (*Rx (t), Ry(t)*) in central injection.

radius is $R_0 = 2\ mm$ into the center of the reinforcement. The flow front progresses in a form of an ellipse characterized by its radii R_x, R_y. The flow front progress of these two radii with the time is shown in Fig. 4 and a comparison between numerical and experimental results is presented. A perfect agreement is obtained between the analytical and the experimental results and the numerical results in the literature. The efficiency of the numerical method developed for the treatment of the flow front is noted. Excellent reproductions of the front shape as well as a good preciseness in the position are observed.

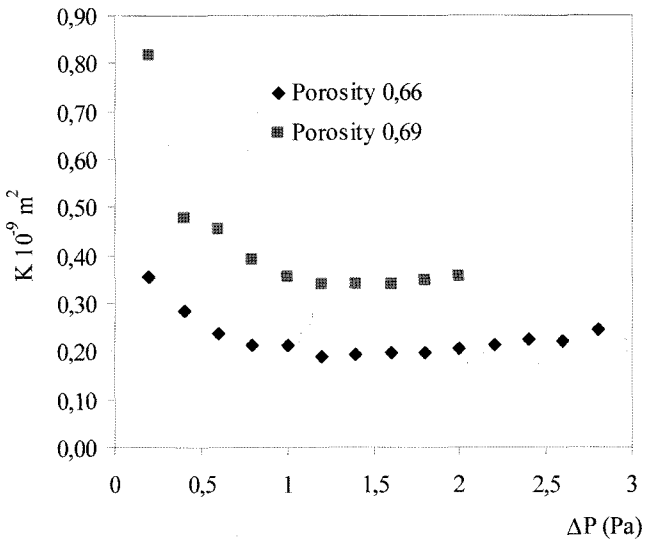

Fig. 5. Evolution of the permeability versus of the pressure drop (linear injection).

5.2. Measurement of permeability

Line injection method makes it possible to measure the permeability in saturated mode and this is generally the most reliable method. We use a glass mat of superficial weight 336.7 g/m^2. The tests are carried out for a line injection with the reinforcement porosities of 0.69 and 0.66. The permeability K is then calculated by the application of the Darcy's law as follows.

$$K_i = \frac{\mu Q_{inj}}{S\phi}\frac{x_f}{\Delta P} \tag{8}$$

where S, μ, ϕ, Q, $\Delta P(t) = P_{inj.}(t) - P_{front}(t)$, x_f are the mold section, the fluid viscosity, the porosity of the reinforcement, the flow rate of injection, the pressure drop (Pa) and the position of the flow front, respectively.

The permeability is measured for a line injection with 20 and 22 plies of reinforcements corresponding to the porosities of 0.69 and 0.66, respectively. During the experiments, the flow rate of injection is constant. We measure the pressure drop (ΔP) and the position of the flow front (x_f) corresponding to the time (t). The permeability K is then calculated (Eq. 8) with the mold section S, the reinforcement porosity and the fluid viscosity μ.

From the results obtained (Fig. (5)), we notice a variation of the permeability according to the pressure drop. Beyond a certain value, this pressure drop becomes almost constant and independent of the pressure to the threshold of developed injection (Liu, 2000).

This variation of the permeability can be explained by a nonlinear behavior of the Darcy law, and also by unsaturation of the medium. It is then necessary to take into account the capillarity effect (paragraph 5.3) which cannot be neglected for certain lengths of the flow front.

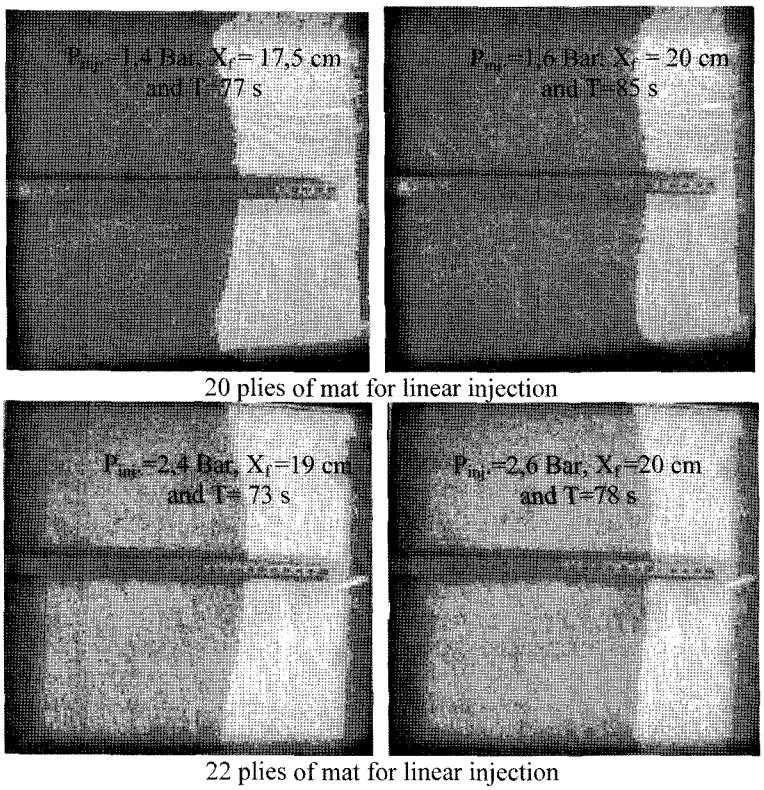

Fig. 6. Evolution of the flow front according to the number of plies, the injection pressure, and the filling time.

The images of the film obtained after soaking are illustrated in Fig. 6. They show the positions of the flow front at different moments. We note that the form of the flow front is rectilinear. Moreover, this study reveals the edge effect which is much lower than that observed in the literature.

The next results presented are obtained for a central injection whose radius of injection port (R_0) is 2 mm. The flow of the injected fluid is realized through an isotropic reinforcement for two injection velocities of 0.35 cm/s and 1.5 cm/s and for a viscosity of 0.21 Pa·s.

The permeability is measured for a radial injection mold with 8 and 9 plies of reinforcements corresponding to the porosities of 0.69 and 0.65, respectively. During the experiments, the pressure drop varies between 0 and 1 bar. For a constant injection velocity (constant flow rate), the pressure drop (ΔP), the position of the flow front (r_f) and the corresponding time (t) are measured. The permeability K is then calculated (Eq. 9) with the radius of injection gate r_0, the porosity of the reinforcement ϕ and the viscosity of the fluid μ.

$$K = \frac{\phi\mu}{2}\frac{(r_f^2 - r_0^2)\ln(r_f/r_0)}{t\,\Delta P} \tag{9}$$

Fig. 7 presents the permeability calculated for the injection pressure measured for two different porosities. The results show that the permeability decreases as the pressure drop increases. Finally, the permeability becomes constant from a pressure drop of 0.25 Bar for the two porosities (Kim *et al.*, 2000). This variation of permeability can be explained by a non linear behavior of Darcy's law, and also by an unsaturation of the reinforcement. The capillarity effect cannot be neglected for a certain length of flow front.

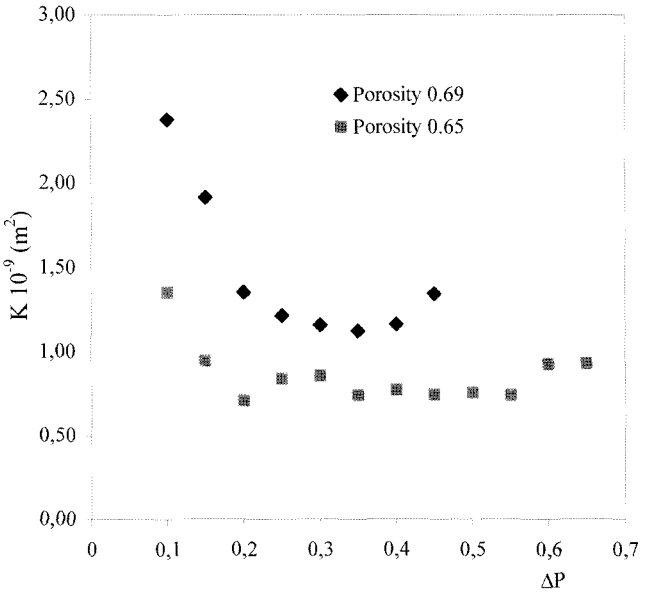

Fig. 7. Evolution of permeability versus the pressure drop (radial injection).

To estimate the capillary effect, the evolution of the capillary number is examined. Several researchers have been concentrated on the one-dimensional form of Darcy's law with the capillary pressure in the flow front (Ahn *et al.*, 1991; Lundström *et al.*, 2000; Lee *et al.*, 2002; Dimitrovova and Advani, 2002, 2004; Hattabi *et al.*, 2005). As a result, the rigorous and precise description of the flow in the neighborhood of the front flow cannot be treated by Darcy's law (Pillai and Advani 1998) basis alone. Indeed, it takes into account only the driving forces due to the pressure or to the compulsory flow rate. At the level of the flow front, it is necessary to take into account the contribution of the capillary pressure, because of the non-wetting of the reinforcement.

5.3. Capillary effects

Wong (1994), defined a flow critical length L_{cv} (cross-over length) to quantify the effect of the capillary pressure. This approach was resumed by Weitzenböck *et al.* (1998), who redefined this length as:

$$L_{cv} = \left(\frac{D_f}{C_a}\right) \tag{10}$$

where C_a is the capillary number and D_f (m) the diameter of the fiber where the pore is placed at the level of the supposed material front subjected to the pressure drop $\Delta P = P_{inj.} - P_{fr.}$ ($P_{inj.}$ pressure of injection and $P_{fr.}$ pressure of the front).

On the basis of Ahn *et al.* (1991), Weitzenböck *et al.* (1998) estimates the capillary pressure P_c (Pa) as a function of the porosity and a parameter F called "Factor of Shape". This factor, often measured experimentally, depends on the alignment of fibers and on the flow direction. Then the capillary pressure for a fibrous reinforcement is defined as:

$$P_c = \left(\frac{F}{D_e}\right)\gamma cos(\theta) \tag{11}$$

where

$$D_e = D_f\left(\frac{\phi}{1-\phi}\right) \tag{12}$$

where γ is the superficial (surface) tension of the fluid (N/m), θ is the contact angle of solid liquid, D_e is the equivalent diameter of the pore and F is the factor of shape ($F=4$ for a flow along the fibers and $F=2$ for a transverse flow in fibers). The advantage of the relation (10) is that it makes it possible to consider a possible affinity between the fibers and the fluid used for the measurement of permeability through the contact angle. The expressions of the critical length calculated for linear and radial flows are (Hattabi *et al.*, 2005):

For linear flow:

$$L_{cv} = D_f\left[\frac{\mu Q_{inj}}{LA\phi^2\gamma cos(\theta)}x_f\right]^{-1} \tag{13}$$

For radial flow:

$$L_{cv} = D_f\left[\frac{\mu Q_{inj}}{2}\frac{(r_f^2 - r_0^2)}{t}Ln\left(\frac{r_f}{r_0}\right)\right]^{-1} \tag{14}$$

Critical length explains the importance of the capillary pressure effect for a given attempt. To estimate the importance of this capillary effect in the radial injection experiment, a modified capillary number is calculated according to the pressure drop, the physical properties of the fluid and to the characteristics of the reinforcement.

By using Darcy's law, this capillary number becomes:

$$C_a = \frac{\mu u}{\gamma cos(\theta)} = \frac{K}{\phi\gamma cos(\theta)}\frac{\Delta P}{L} \tag{15}$$

where u is the relative flow velocity when the fluid per-

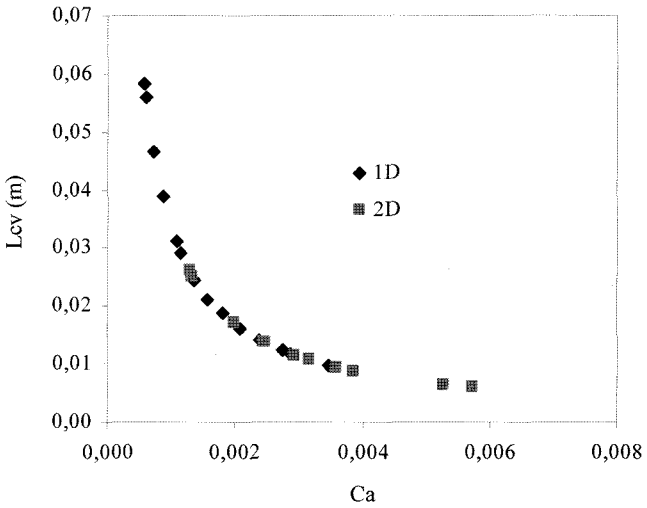

Fig. 8. Evolution of the critical length vs the capillary number for unidirectional and radial injections.

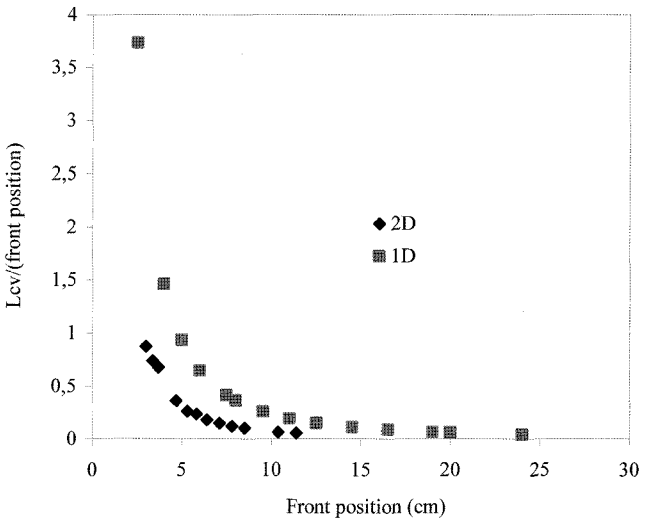

Fig. 9. Evolution of the ratio of the critical length and the position of the front for unidirectional and radial injections.

meates in the dry fibers, $\frac{\Delta P}{L}$ is the pressure gradient through the reinforcement of permeability K. Eq. (15) was also used by (Foley and Gutowski, 1991), who found a transition where permeability decreased at a capillary number of the order of 0.01.

The analysis of the flow through a fibrous medium (particularly within the framework of the measurement of the permeability) can be examined by using critical length, which measures the importance of the capillary effect during the impregnation of the reinforcement. This effect depends on the capillary number and on the type of reinforcement.

Afterward, the values used in this study are the injection velocity $U_{inj.} = 0.35\ cm/s$ or $U_{inj.} = 1.5\ cm/s$, the factor of shape $F = 2$, the viscosity $\mu = 0.12\ Pa \cdot s$ (glycerin), the superficial (surface) tension of the fluid $\gamma = 60\ 10^{-3}\ N/m$ (Patel and Lee, 1995) and the contact angle between solid and liquid $\theta = 0^{\circ}$ (Patel and Lee, 1995).

The evolution of the critical length of the flow according to the capillary number for two configurations of linear and radial flows is presented in Fig. 8. Results show that the flow critical length decreases considerably when the capillary number increases. It is noted that from a capillary number of the order of 10^{-4}, the flow critical length becomes very short. This means a transition toward the saturation.

Fig. 9 represents the ratio between the critical lengths of the flow and the position of the front according to the kinetics of the front for two flow configurations (linear and radial). At the beginning of the experiments, an important decrease in the ratio is observed, which is more important for linear flow than for radial flow.

The importance of the capillary effect depends on the parameters of the molding. This effect decreases if the filling time decreases; that is, if the pressure where the debit of injection increases. It also decreases if the porosity decreases. The curves also show that this effect is important at the beginning of injection and decreases with the length of the flow front (Fig. 9).

6. Conclusions

In this study, a numerical model for isothermal mold filling simulation for the RTM process was developed. A finite difference method associated with a curvilinear, evolutionary meshing and adapted to the geometry of the saturated zone was employed. The numerical simulation results obtained showed a perfect agreement with the analytical, experimental and numerical results from the literatures. The efficiency of the numerical model developed in the treatment of the front in this type of flow was noted. An excellent reproduction of the shape of the front as well as a good preciseness in the position was obtained. On the other hand, a simple experimental assembly was devised to measure the pressure and the flow front to calculate the permeability for different porosities. The purpose of the work was to estimate the importance of the capillary effect for the tests. This capillary effect was modeled by the critical length whose expression was calculated in linear and radial flow. The obtained results showed that this effect is important at the beginning of the injection and becomes unimportant for a pressure drop of the order of 0.25 Bar. The used assembly and the chosen parameters of molding made the measurement of permeability reliable.

References

Ahn, K. J., J. C. Seferis and J. C. Berg, 1991, Simultaneous measurement of permeability and capillary pressure of thermosetting, *Polymer Composites* **12**(3), 146-152.

Bruschke, M. V. and S. G. Advani , 1990, A finite element/control volume approch to mold filling in anisotropic porous media, *Polymer composites* **11**, 398-405.

Dimitrovova, Z. and S. G. Advani, 2002, Analysis and characterization of relative permeability and capillary pressure for free surface flow of a viscous fluid across an array of aligned cylindrical fibers, *Journal of Colloid and Interface Science* **245**(2), 325-337.

Dimitrovova, Z. and S. G. Advani, 2004, Mesolevel analysis of the transition region formation and evolution during the liquid composite molding process, *Computers and Structures* **82**, 1333-1347.

Foley, M. F. and T. Gutowski, 1991, *23rd International SAMPE Technical Conference* **23**, 326-340.

Gauvin, R. and F. Trochu, 1993, Comparaison between numerical and experimental results for mold filling in resin transfer molding, *Plastics, rubber and composites processing and applications* **19**(3), 151-157.

Gouley, G., 1995, Etude des écoulements dans les procédés d'injection de résine sur renfort, PhD thesis, University of sciences and technology of Lille Flandres Artois.

Hattabi, M., J. Echaabi, M. O. Bensalah, J. Bréard and A. Saouab, 2005, Analysis flow during on-line injections and radial application in the measure of permeability, *Journal of Reinforced Plastics & Composites* **24**, 1909-1920.

Hattabi, M., I. Snake, J. Echaabi and M. O. Bensalah, 2005, Simulation du front d'écoulement dans les procédés de moulage des composites liquides, *Comptes Rendus de Mécanique*, Ed Elsevier, 585-591.

Kim, B. Y., G. J. Nam, H. S. Ryu and J. W. Lee, 2000, Optimization of filling process in RTM using genetic algorithm, *Korea-Australia Rheology Journal* **12**(1), 83-92.

Lee, G. W., N. J. Lee, J. Jang, K. J. Lee and J. D. Nam, 2002, Effects of surface modification on the resin-transfer moulding (RTM) of glass-fibre/unsaturated-polyester composites, *Composites Science and Technology* **62**, 9-16.

Liu, X. L., 2000, Isothermal flow simulation of liquid composite molding, *Composites Part A: Applied Science and Manufacturing* **31**(12), 1295-1302.

Lundström, T. S., R. Stenberg, R. Bergström, H. Partanen and P. A. Birkeland, 2000, In-plane permeability measurements: a Nordic round-robin study, *Composites Part A: Applied Science and Manufacturing*, **31**(1), 29-43.

Patel, N. and L. J. Lee, 1995, Effects of fiber mat architecture on void formation and removal in liquid composite molding, *Polymer Composites* **16**(5), 386-399.

Pillai, K. L. and S. G. Advani, 1998, Numerical simulation of unsaturated flow in woven fiber preform during the resin transfer molding process, *Polymer Composites* **19**(1), 71-80.

Saouab, A, 1991, Génération de maillage adaptatifs par une méthode variationnelle, thesis PhD thesis, University of the Rouen.

Shojaei, A., S. R. Ghaffarian, S. M. H. Karimian, 2002, Numerical simulation of three-dimensional mold filling process in resin transfer molding using quasi-steady state and partial saturation formulations, *Composites Science and Technology* **62**, 861-879.

Weitzenböck, J. R., R. A. Shenoi and P. A. Wilson, 1998, Measurement of threedimensional permeability, *Composites-Part A: Applied Science and Manufacturing* **29**A(1-2), 159-169.

Wong, P. Z., 1994, Flow in porous media: permeability and displacement patterns, *MRS Bull.* **19**(5), 32-38.

Young, W. B., K. Han, L. H. Fong, L. J. Lee and M. J. Liou, 1991, Flow simulation in molds with preplaced fiber mats, *Polymer Composites* **12**(6), 391-403.